AJNR

MR Evaluation of Large Intracranial Aneurysms Using Cine Low Flip Angle Gradient-Refocused Imaging

Jay S. Tsuruda, Van V. Halbach, Randall T. Higashida, Alexander S. Mark, Grant B. Hieshima and David Norman

AJNR Am J Neuroradiol 1988, 9 (3) 415-424
http://www.ajnr.org/content/9/3/415

MR Evaluation of Large Intracranial Aneurysms Using Cine Low Flip Angle Gradient-Refocused Imaging

Jay S. Tsuruda[1,2]
Van V. Halbach
Randall T. Higashida
Alexander S. Mark
Grant B. Hieshima
David Norman

MR imaging has proved to be useful in evaluating large intracranial aneurysms. The parent artery and patent lumen can be identified as flow voids and differentiated from thrombus. However, in the presence of slow flow, even-echo rephasing, and motion artifact, increased intraluminal signal may be present, which may be difficult to distinguish from thrombus. Aneurysms are also dynamic lesions and exert pulsatile mass effect on adjacent structures. Further definition of vascular anatomy and physiology may aid in therapeutic planning and assessment. Cine MR is a new technique using a movie loop of sequential GRASS (gradient-recalled acquisition in the steady state) images obtained during various points in the cardiac cycle. The combination of GRASS images and cardiac gating thus allows cinegraphic display of vascular structures. A comparison of this method with routine T1- and T2-weighted MR imaging and angiography was made in a group of 13 patients with intracranial aneurysms greater than 1.5 cm in diameter. Eight of these patients underwent transvascular detachable balloon occlusion. With cine MR, flowing blood has high intensity due to flow-related enhancement. Turbulent and high-velocity flow can be recognized on the basis of signal loss, which occurs during systole. Thrombus demonstrated variable signal intensity, which remained unchanged during the cardiac cycle. Compared with routine MR sequences, there was less image degradation from phase-encoding artifacts and improved visualization of the neck of the aneurysm. Pulsatile mass effect was uniquely assessed. After transvascular embolization, cine MR demonstrated improved conspicuity of acute thrombus and higher contrast between flowing blood and the occlusion balloon when compared with routine MR. Confirmation of flow within the parent vessel, residual aneurysm lumen, and distal arterial branches is possible. If the parent vessel was occluded, cine MR yielded greater information than angiography.

Cine MR provides additional anatomic and physiologic data in the evaluation and assessment of therapy of intracranial aneurysms. Information can be obtained that is not available with either routine MR or angiography. The inherent limitations of this new technique include partial-volume artifacts, less than optimal flow-related enhancement or spatial resolution, and poor data acquisition due to cardiac arrhythmias.

This article appears in the May/June 1988 issue of *AJNR* and the July 1988 issue of *AJR*.

Received September 11, 1987; accepted after revision December 28, 1987.

Presented at the annual meeting of the American Society of Neuroradiology, New York, May 1987.

[1] All authors: Department of Radiology, Diagnostic and Interventional Neuroradiology Section, University of California, San Francisco, 505 Parnassus Ave., San Francisco, CA 94143-0628.

[2] Present address: MR Imaging Laboratory, Huntington Medical Research Institutes, 10 Pico St., Pasadena, CA 91105. Address reprint requests to J. S. Tsuruda.

***AJNR* 9:415–424, May/June 1988**
0195–6108/88/0903–0415

The evaluation of intracranial aneurysms by MR has been described. MR has several known advantages over both angiography and contrast-enhanced CT. These advantages include identification of signal void within the patent lumen [1–5], laminated thrombus [4], adjacent parenchymal edema and hemorrhage [2, 4], and parent vessel [4], as well as the definition of an extraaxial location with mass effect [5]. For these reasons MR may be more specific in characterizing these lesions [4, 5]. The patent lumen of the aneurysm can be identified on routine MR sequences by high-velocity signal loss (resulting from time-of-flight effects) or by turbulence. However, in the presence of slow flow and/or even-echo rephasing [2, 5], distinguishing flowing blood from thrombus may be difficult. On the other hand, calcium in the aneurysm wall may be confused with flow void. If the residual vascular channel is eccentrically located with associated thrombus, a giant aneurysm may be mistaken for an arteriovenous malformation [3]. Giant aneurysms have a variable incidence of associated subarachnoid hemorrhage and are usually

manifested clinically as a progressive space-occupying mass [6–8]. Aneurysms are dynamic lesions that exert pulsatile, expansive pressure on adjacent brain parenchyma and cranial nerves, contributing to the patient's symptoms [9]. With the advent of transvascular balloon occlusion techniques, additional anatomic and physiologic information gained by MR may be helpful in therapeutic planning and assessment.

Cine MR has recently been used to evaluate dynamic cardiac function in normal and diseased hearts [10–12]. With this technique, images are rapidly acquired with gradient-recalled echoes, short repetition times (TRs), and low flip angles [13, 14]. When combined with ECG gating, images are obtained at specific points during the cardiac cycle, which, when displayed as a cine loop, simulate real-time cardiac imaging [10]. The purpose of our study was to assess the use of cine MR in conjunction with routine MR and angiography in the evaluation of large and giant aneurysms before and after transvascular embolic therapy.

Subjects and Methods

Thirteen patients, eight female (mean age, 53) and five males (mean age, 35), with an age range of 7–73 years were included in this series. Aneurysms with a cross-sectional diameter of greater than 2.5 cm were considered to be giant, and those in the range of 1.5–2.5 cm were considered to be large [7]. Eight patients had giant aneurysms (range, 2.6–4.7 cm) and four had large aneurysms (range, 1.6–2.6 cm). One additional patient with a 0.9-cm aneurysm was included in the large aneurysm group. The aneurysms involved the petrosal and cavernous segments of the carotid artery in one patient, cavernous carotid artery in three, carotid-ophthalmic artery in one, supraclinoid carotid artery (including the origin of the posterior communicating artery and carotid bifurcation) in two, middle cerebral trifurcation in two, anterior cerebral artery in one, basilar artery tip in two, and posterior inferior cerebellar artery in one. In one patient, the aneurysm had a posttraumatic origin after repair of a carotid-cavernous fistula.

Eight of the patients were treated by transvascular occlusion using a detachable balloon solidified with a hydrophilic polymer, 5-hydroxyethyl methacrylate (HEMA) [15]. In three of these patients, either single or multiple balloons were detached directly into the lumen of the aneurysm in an attempt to preserve the parent vessel. In the remaining five patients, the parent artery was occluded by using a detachable balloon. In one instance, multiple Gianturco coils were placed in the internal carotid artery proximal to the detached balloon. One patient underwent surgical clipping. Four patients were not treated because of nearly complete, spontaneous thrombosis of the aneurysm in two patients and fresh thrombus within the aneurysm in one. The remaining patient had an asymptomatic large supraclinoid aneurysm and was followed electively.

MR was performed in all patients on a 1.5-T GE superconducting system using a standard whole-volume head coil. Routine MR sequences were first performed using a multisection, single- or multi-spin-echo technique in both the sagittal and axial planes. T1-weighted 600/20 (TR/TE) and T2-weighted 2000/35, 70 MR sequences were performed in the sagittal and axial planes, respectively. In selected cases, additional T1-weighted coronal or axial images were obtained. Slice thickness was 5 mm in all cases with an interslice gap of either 1 mm on the T1-weighted sequence or 2.5 mm on the T2-weighted sequence; 128 or 256 phase-encoded projections with one or two excitations with a 20- or 24-cm field of view were used.

Immediately after routine MR, the cine MR study was performed using GRASS (gradient-recalled acquisition in the steady state). This protocol is essentially the same as for cardiac cine MR with only a few modifications, as detailed in previous reports [10, 12]. A flip angle of 30°, TR = 21, and a gradient-refocused echo with TE = 12.5 were used. Data acquisition was continuous during a simultaneous recording of the ECG signal performed with standard four-lead chest electrodes. The phase-encoding gradient was advanced with each detected R-wave for a total of 128 beats, corresponding to an equal number of phase-encoded projections. Unlike standard cardiac-gated images, the TR remained independent of the heart rate. The number of time frames per cardiac cycle is dependent on the length of the R-R interval and number of slice positions acquired during a single data collection [12]. Since there is beat to beat variation of the R-R interval length, linear interpolation was used to correct for these time differences prior to image reconstruction. A typical cine MR acquisition consisted of four contiguous 5-mm-thick slices with a coverage of 20 mm. Eight to 12 time frames were obtained during each R-R interval at each slice position with an approximate time resolution of 80 msec (Fig. 1A). Since two excitations were used, a total of 256 beats (128 phase-encoded projections × 2) are observed, corresponding to an imaging time of 3.6 min for a heart rate of 70. A 24-cm field of view with an interpolated 256 × 256 display was used, yielding a 0.94 × 1.88 mm pixel size. In each case, the aneurysm was studied in all three orthogonal planes. The entire study, consisting of the routine and cine MR images, can be performed in 1 hr.

Routine and cine MR was performed before and after endovascular therapy in three patients, before therapy only in three other patients, and after therapy only in two patients. Arteriography using subtraction and magnification techniques was performed in 11 of 13 patients within 24 hr of the MR study. In the remaining two patients, arteriography was obtained earlier than 1 week before MR. Nonenhanced and enhanced CT scans were available for comparison in seven patients. A comparative analysis of arteriography and routine and cine MR studies was made. We specifically studied vascular flow, associated turbulence, identification of the neck of the aneurysm, the presence of thrombus, location of the occlusion balloon, and detection of associated parenchymal abnormalities. The findings are discussed separately in the pre- and posttherapy groups.

Results

Pretherapy

Blood Flow. Of the study population of 13 patients, a pretherapeutic routine and cine MR was performed in 11. In this subgroup, routine MR demonstrated intraluminal blood flow in nine. In five of these nine patients, characteristic homogeneous flow void was present. In the remaining four patients, intraluminal signal mimicking thrombus was identified. The signal represented slow flow and/or motion artifact (Figs. 1C, 2A, and 2B) in three patients. In one case, both motion artifact and even-echo rephasing was noted (Fig. 3C). The degree of phase artifact often varied between the T1- and T2-weighted studies and with the plane of section. In the same group of nine patients, cine MR depiction of flowing blood in either the aneurysm lumen or parent artery had higher signal intensity than did brain parenchyma, CSF, or the majority of thrombi. The distribution of high intraluminal signal was variable and primarily dependent on two factors: the relative volume of flowing blood and the phase of the cardiac cycle. High signal was most pronounced in regions of high

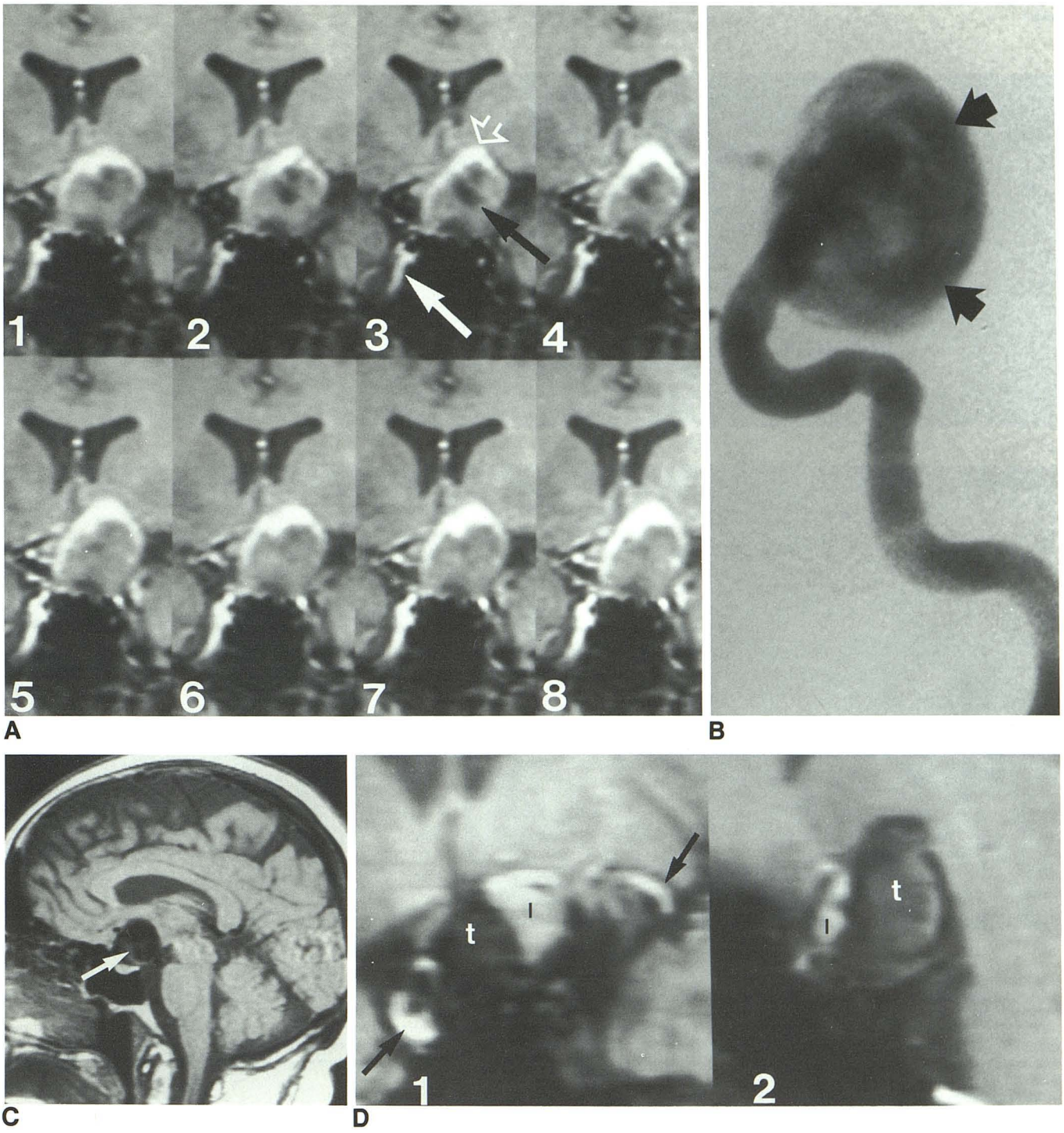

Fig. 1.—54-year-old woman with 2.5-cm left nonthrombosed, supraclinoid carotid artery aneurysm pre- (*A–C*) and post- (*D*) parent artery balloon embolization.

***A*, Series of eight cine coronal images obtained at a single-slice position through mid-portion of untreated aneurysm. The study begins with image 1,2 5 msec after the R wave and therefore represents late diastole. Each subsequent image, obtained at 80-msec intervals, corresponds to a later period during the cardiac cycle: image 2 (early systole), image 4 (mid to late systole), and image 7 (diastole). Images can be displayed as a movie loop, and playback speed is readily adjusted by the viewer. In this fashion, any time-dependent changes become more obvious. Generally, four slice positions are obtained during a single acquisition and simultaneously displayed on video monitor (see Fig. 2E). During systole, a region of intraluminal signal dropout can be identified (*black arrow*) corresponding to turbulence and/or high-shear laminar flow (see Discussion). Accompanying upward deformity (*open arrow*) of superior wall of aneurysm is present and corresponds to region of highest blood flow as depicted by a crescentic band of high intensity. Note high flow in right cavernous carotid artery (*white arrow*). This can also be identified in the parent left carotid artery but was better seen in the slice position 5 mm anteriorly (not shown).**

***B*, Correlative left internal carotid arteriogram obtained in lateral view. Note area of highest contrast density or flow along periphery (*arrows*). The earliest image after injection (not shown) demonstrated a jet of contrast directed toward superior dome of aneurysm.**

***C*, T1-weighted sagittal MR image (SE 600/20) shows aneurysm with heterogeneous intraluminal signal (*arrow*), mimicking thrombus, representing slow flow and/or phase-encoding artifact.**

***D*, 72 hours after parent artery embolization, repeat cine MR depicts partial thrombosis of lumen of aneurysm. Both coronal image 1 and sagittal image 2 represent late systole. Low-intensity thrombus (t) and residual high-intensity lumen (l) are present. Flow can be seen in contralateral internal carotid and ipsilateral middle cerebral arteries (*arrows*). Pulsatile motion was no longer present.**

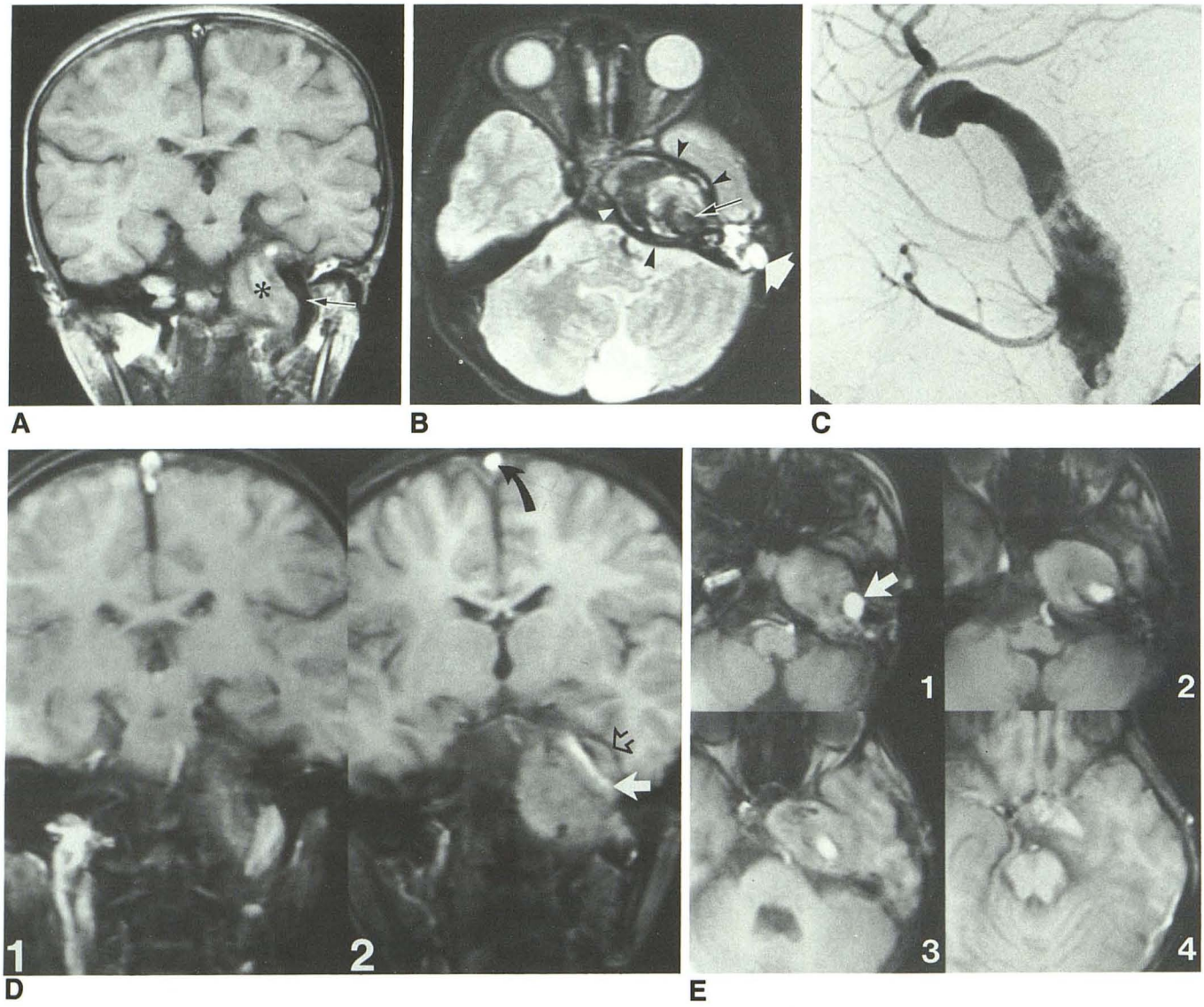

Fig. 2.—Giant, partially thrombosed left petrosal and cavernous segments of carotid artery aneurysm in 7-year-old boy.

***A*, T1-weighted coronal MR image (SE 600/20) shows extraaxial, heterogeneous skull base mass filled with thrombus (*asterisk*) nearly isointense with brain parenchyma. An eccentric lumen with minimal heterogeneous phase artifact (*arrow*) is present.**

***B*, T2-weighted axial MR image (SE 2000/70) shows heterogeneous, decreased signal intensity within thrombus surrounded by well-circumscribed rim of low signal (*arrowheads*) possibly representing hemosiderin deposition since calcium was not present on CT (not shown). The lumen (*long thin arrow*) has intermediate signal due to slow flow as noted on arteriogram and is difficult to distinguish from thrombus. High-intensity fluid is seen in multiple mastoid air cells (*short wide arrow*).**

***C*, Correlative left lateral common carotid arteriogram shows fusiform vascular channel within aneurysm.**

***D*, Cine MR coronal images during late systole at two contiguous slice positions shows high-intensity flowing blood within vascular channel (*closed arrow*). Low-intensity rim (*open arrow*) is present medial to displaced left temporal lobe. Note also the high-intensity flow within superior sagittal sinus (*curved arrow*).**

***E*, Axial cine MR sections at four slice positions acquired during systole. The vascular channel (*arrow*) has even higher intensity relative to surrounding brain parenchyma and thrombus when compared with Fig. 2D, since flow is perpendicular rather than parallel to plane of section. Thrombus is isointense when compared with brain parenchyma. Regions of low intensity within thrombus on T2 weighting (Fig. 2B) are not identified.**

flow (Fig. 1A), especially in the neck of the aneurysm or within the lumen of the aneurysm immediately adjacent to this area (Fig. 3B). Occasionally, a jet or wave of high signal extended from the neck of the aneurysm into the lumen to admix with blood of slightly lower intensity. Elevated intraluminal signal was seen throughout the cardiac cycle but was more pronounced during mid and late systole and early diastole, depending on the degree of associated turbulence.

The intravascular signal intensity was also dependent on the plane of section. The greatest signal occurred when flowing blood was perpendicular to the imaging plane (Figs. 2D and 2E). Lower intraluminal signal intensity occurred if the

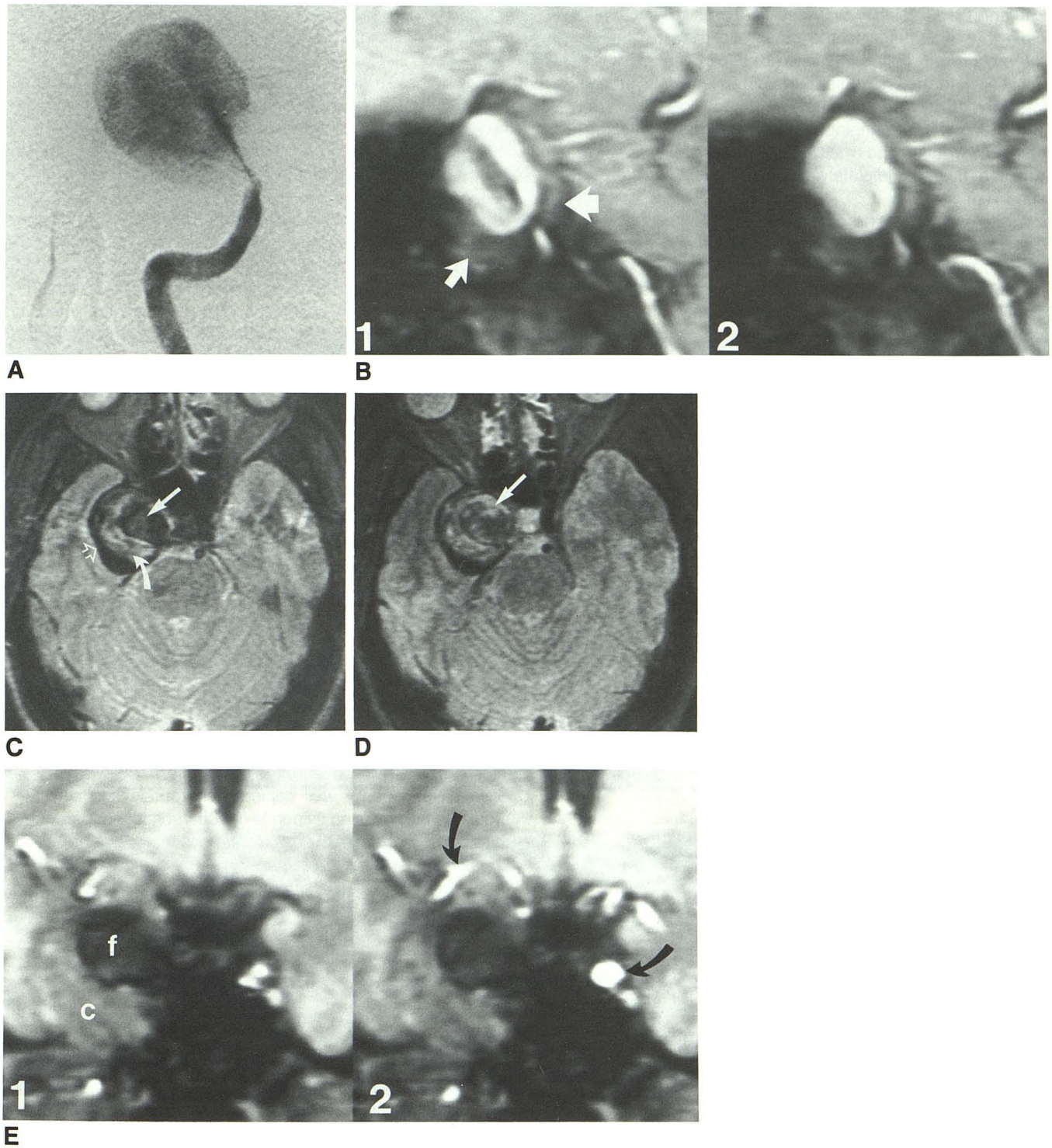

Fig. 3.—42-year-old man with 3.8-cm partially thrombosed right cavernous carotid artery aneurysm pre- (*A–C*) and post- (*D*, *E*) parent artery balloon embolization.

***A*, Oblique right internal carotid arteriogram demonstrates a jet of contrast filling a partially opacified lumen.**

***B*, Sagittal cine MR images corresponding to systole (image 1) and diastole (image 2) show a similar jet of turbulent blood as a spindle-shaped region of low signal during systole only. Intermediate-signal-intensity thrombus is seen inferiorly and posteriorly (*arrows*).**

***C*, T2-weighted axial MR image (SE 2000/70). Aneurysm has increased intraluminal signal due to phase-encoding artifact and even-echo rephasing (*straight arrow*), mixed-signal-intensity thrombus (*curved arrow*), and low-intensity rim (*open arrow*), which was partially calcified on CT (not shown).**

***D*, 24 hr after proximal artery occlusion, a repeat T2-weighted axial MR study (SE 2000/70) reveals fresh thrombus with mixed signal intensity (*arrow*). Phase artifact is no longer present.**

***E*, Corresponding coronal cine MR 24 hr after occlusion during systole (image 1) and diastole (image 2). Fresh thrombus (f) has distinctly lower intensity compared with chronic, presumably organized, thrombus (c). High intensity is seen within contralateral internal carotid and ipsilateral middle cerebral arteries (*curved arrows*) but not in parent cavernous carotid artery. Note that higher intraarterial signal is seen during diastole (image 2) due to less turbulent flow.**

entering blood velocity was decreased or "diluted" within a capacious aneurysm. In the other two patients in the pretherapy group, routine MR failed to depict accurately intraluminal flow. In the first patient, the persistently elevated signal intensity on all sequences was due to slow flow (Fig. 4), correlating with the angiographic findings. In the second patient, both routine and cine MR missed a small residual lumen within a nearly completely thrombosed 2.5-cm cavernous aneurysm.

Turbulence. Regions of high flow were accompanied by discrete areas of signal dropout, presumably representing random motion (turbulence) and/or shear effects (Figs. 1A and 3B). These areas of signal dropout also varied in a time-dependent fashion. They were seen predominantly during the initial images after the R-wave, corresponding to early and mid systole. During diastole, this signal loss either decreased significantly or disappeared, presumably due to less random flow. Because of this time dependency, turbulent flow could be distinguished from thrombus, which did not change in signal intensity throughout the cardiac cycle. Pansystolic turbulent flow was also seen within major arterial structures such as the internal carotid artery and M1 segments of the middle cerebral arteries. In these structures, a more uniform high intraluminal signal was noted during diastole (Fig. 3E).

Aneurysm Neck and Wall Motion. The regions of high flow with associated turbulence seen on cine MR correlated with the jet effect of contrast, originating from the neck of the aneurysm and filling the lumen of the aneurysm on arteriography (Fig. 3B). As a result, cine MR depicted this region more accurately than did routine MR. High-intensity flowing blood was noted to traverse the aneurysm and strike the opposite wall, resulting in its outward expansion and pulsatile mass effect on adjacent brain tissue. This deformity was especially noticeable in one nonthrombosed giant aneurysm (Fig. 1A).

Thrombus. Thrombus was identified in eight of 11 patients on routine MR. The thrombi appeared as areas of heterogeneous mixed signal intensity on all pulsing sequences. The thrombus was iso- to hyperintense on T1-weighted images. Hyperintensity within the thrombus, when present, had a varying thickness and was not only confined to an inner rim immediately adjacent to the patent lumen (Fig. 4). In three patients, the most peripheral rim of thrombus demonstrated areas of hyperintensity.

Thrombus appeared heterogeneous with mixed signal intensity on routine T2 weighting. The predominant intensity was decreased especially on the most heavily T2-weighted image (SE, 2000/75) (Figs. 2B and 5B). However, irregular regions of iso- and hyperintensity (when compared with brain parenchyma) were also present. A frequent finding was a peripheral rim of low intensity better noted on the T2-weighted images (Figs. 2B, 3C, and 3D). Peripheral calcification, identified on CT, could account for portions of the signal loss.

On cine MR, thrombi were isointense or had varying degrees of hypointensity compared with surrounding brain parenchyma. The low-intensity rim seen on routine T2-weighted images was also seen. On cine MR, the regions of hyperintensity on T1-weighted images were also shown to be hyperintense on cine MR. In one case, distinction between high-intensity thrombus and flowing blood was difficult (Fig. 4).

Parenchymal Changes. Adjacent parenchymal changes were identified in four patients before therapy as regions of elevated intensity and mild hypointensity on the T2- and T1-weighted images, respectively (Fig. 5B). On the corresponding cine MR images, absent or subtle low-intensity changes were noted in a similar distribution. Mass effect secondary to edema was equally well depicted on routine and cine MR studies. There was no evidence of subarachnoid or parenchymal hemorrhage on either the routine or cine MR. The lack of hemorrhage was in agreement with the clinical histories of the patients in the study group.

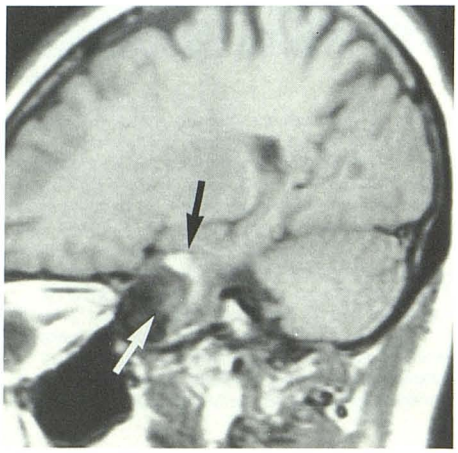

Fig. 4.—54-year-old woman with 3.5-cm right carotid-ophthalmic artery aneurysm. T1-weighted sagittal MR image (SE 600/20). Persistent heterogeneous signal intensity (*white arrow*) is noted within patent lumen due to slow flow. Similar findings were also noted on T2-weighted sequences (not shown). A thick rim of high intensity (*black arrow*) possibly representing methemoglobin (see also Fig. 5C), which can be confused with flowing blood on cine MR, is seen within thrombus.

Posttherapy

Six patients were examined after embolic therapy. In three cases the balloon was within the aneurysm, and complete thrombosis was confirmed by angiography in two of these patients. The intraaneurysmal balloons had a low signal intensity on routine MR and could not be distinguished from flowing blood (Fig. 5E). Although the HEMA-filled balloons contained small amounts of solidified ferrous ammonium sulfate, distortion of the surrounding parenchyma secondary to metallic artifact was not present. Similar low signal intensity of the balloon was also seen on cine MR; however, high-signal flowing blood was readily identified adjacent to the balloon in either the patent lumen of the aneurysm or the parent vessel (Fig. 5F). In the remaining three patients, the parent artery was embolized. Cine MR was able to confirm the loss of high-signal blood flow within the occluded artery in all cases and

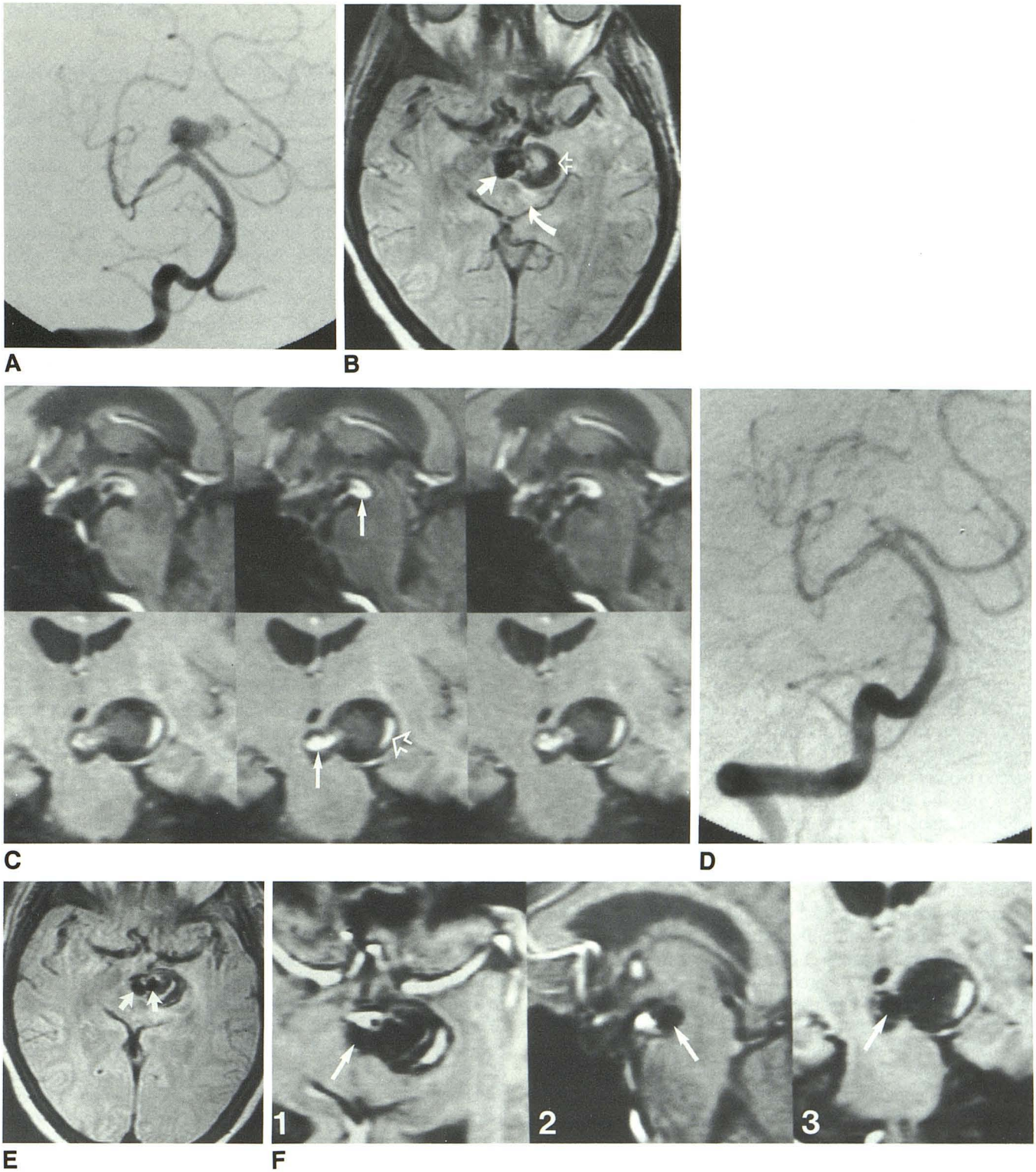

Fig. 5.—61-year-old woman with 3.0-cm partially thrombosed aneurysm of basilar tip pre- (*A–C*) and post- (*D–F*) intraaneurysmal balloon embolization.

***A*, Right vertebral arteriogram in Towne projection demonstrates filling of irregular basilar tip aneurysm.**

***B*, T2-weighted axial MR image (SE 2000/35). Flow void is seen within patent lumen (*straight arrow*) with eccentric, mixed-signal-intensity thrombus (*open arrow*). Minimal adjacent high-intensity edema is present (*curved arrow*).**

***C*, Cine MR images in sagittal (*top row*) and coronal (*bottom row*) planes. The first column corresponds to early systole, the second column to late systole, and the third column to diastole. High signal within patent lumen (*closed arrows*) is seen. Variability of signal intensity is present depending on phase of cardiac cycle and extent of turbulence. The majority of thrombus has low intensity compared with surrounding brain; however, a peripheral zone of high signal (*open arrow*) can be seen of similar intensity to flowing blood. This zone did not opacify on arteriography, remained unchanged during the cardiac cycle, and presumably represents a methemoglobin rim within thrombus.**

***D*, After intraaneurysmal balloon embolization, repeat right vertebral arteriogram reveals complete occlusion of lumen of aneurysm.**

***E*, T2-weighted axial MR image (SE 2000/35). Two HEMA-filled balloons (*arrows*) of low signal intensity are identified. Because HEMA-filled balloons and flowing blood may have identical signal void, routine MR is not able to distinguish between these two entities.**

***F*, Repeat diastolic cine MR in axial (image 1), sagittal (image 2), and coronal (image 3) planes. Low intensity can be seen within HEMA-filled balloons (*arrows*), which is readily distinguished from high signal within patent distal basilar artery.**

demonstrate collateral filling distally (Figs. 1D and 3E). In one case, cine MR could clearly distinguish acute thrombus from presumably organized clot 24 hr after occlusion (Fig. 3E).

Discussion

The utility of conventional MR in the diagnosis of giant aneurysms has recently been discussed in detail [4, 5]. Improved specificity is provided by MR because of its superior characterization of flowing blood, identification of an extraaxial location, and detection of thrombus. Rapidly flowing intraluminal blood appears as signal void due to either phase dispersion or time-of-flight effects (caused by spins flowing out of the imaging slice between selective 90° and 180° pulses) resulting in high-velocity signal loss [16–18]. However, in a significant number of cases, intraluminal signal of intermediate to high intensity could be identified persistently on both T1- and T2-weighted images, mimicking thrombus [5]. Possible causes of this finding include phase-encoding artifact, slow flow, flow-related enhancement (entry slice phenomenon), or even-echo rephasing [17, 19]. The addition of flow-sensitive sequences may add to the diagnostic accuracy in evaluating intracranial aneurysms and may contribute to therapy planning and posttherapeutic assessment.

Recent application of cine MR in the evaluation of the heart has shown promising results in the assessment of cardiac anatomy and function, including chamber size, wall motion and thickening, valvular heart disease, and turbulent flow [10–12]. The basis of this imaging technique is the application of partial flip angles with gradient-refocused echoes for rapid image acquisition [13, 14]. Relatively high signal intensity of flowing blood is caused by the inflow of moving, unsaturated spins into the imaging plane relative to stationary, partially saturated spins [16]. This phenomenon of flow-related enhancement is accentuated with short repetition times and high velocities, and is greatest when motion is perpendicular to the sensitive slice [14, 17].

Gradient-refocused echoes have greater sensitivity for fast flow in comparison with conventional 180° spin echoes for several additional reasons. First, there is less dephasing of moving protons as compared with spin echoes [20], and, second, spins that are initially excited by the 90° pulse and move away from the slice may still have signal, since gradient refocusing is not slice-selective [21]. As a result, velocity sensitivity over a "greater dynamic range" is achieved [22]. The phase-encoding artifact seen as elevated intraluminal intensity on routine MR was less apparent. In part, reduction of phase artifact was secondary to decreased sensitivity to flow parallel to the plane of section and the application of flow-motion-compensation gradients [14, 23]. Because of software limitations, we were unable to apply flow-compensation gradients to the routine spin-echo images.

Use of the appropriate flip angle may also be an important factor in determining adequate contrast between stationary and moving spins. By increasing the flip angle, contrast is increased by decreasing the relative intensity of the stationary spins and by increasing the magnetization of entering spins [14, 21, 24]. However, as the flip angle approaches 90°, we have noted greater flow artifacts and decreased intraluminal signal intensity. Similar findings were noted in cardiac imaging, possibly caused by increased turbulence or in-plane flow [21]. The use of a 30° flip angle is a compromise between having sufficient contrast without excessive flow artifact. Longer gradient echo times (TE) may also improve contrast in a similar fashion. Although we did not verify experimentally this sequence on any of our patients, there are several potential disadvantages in using long TEs. First, by prolonging the TE, fewer images can be obtained during the R-R interval, resulting in reduction of the temporal resolution. Second, the signal-to-noise will be diminished. Finally, greater sensitivity to magnetic field inhomogeneities is encountered with longer TEs [25]. In vivo variations in tissue magnetic susceptibility may contribute to this inhomogeneity and may be significant at the skull base and adjacent to large vascular structures [26]. As a result, image distortion may occur, possibly affecting the detailed anatomic evaluation of the circle of Willis.

Turbulence (random motion) can be observed with cine MR both in vivo and experimental studies as discrete areas of signal drop-out [10, 20]. These areas of signal loss result from destructive phase interference from both spatial variations in velocity and temporal variations; that is, acceleration [18]. On cardiac cine MR, turbulence associated with regurgitant valvular disease appears as a fan or spindle-shaped region of signal dropout [10]. Similar findings are demonstrated on cine MR views in some aneurysms, when filling across a relatively narrow neck of the aneurysm creates a jet of blood, as seen with angiography. Shear effects from nonturbulent flow may contribute to signal loss at the interface between stationary and moving blood provided that laminar flow is present. We felt that the relative contribution of shear effects was much less than random motion. Therefore, for simplification, signal dropout is thought to result primarily from turbulence.

The preceding discussion demonstrates that limited flip angle, gradient-refocused imaging may accurately indicate high velocity and/or turbulent flow states. An added advantage is the ability to obtain time-dependent physiologic analysis of flow through the cardiac cycle. Since rapid periodic motion exists, physiologic analysis can be achieved by combining short imaging times with ECG gating. A large number of identical projections at multiple slice positions can be obtained over a period of several hundred cardiac cycles, corresponding to the number of phase-encoded projections and necessary excitations [14]. The resulting temporal resolution is similar to angiography and allows for cinematic display with improved edge detection of the interface between moving and stationary spins [10]. Pretherapeutic assessment of aneurysms is enhanced by the application of cine MR. Areas of flow can be recognized by demonstrating variable high intraluminal velocities. Turbulent flow is recognized as time-dependent phase dispersion during the cardiac cycle. Similar to cardiac wall motion, pulsatile motion of the aneurysm wall and its mass effect on the adjacent brain parenchyma can be analyzed. Thrombus can be diagnosed easily on cine MR because it has no pulsatile motion and therefore remains unchanged during the cardiac cycle.

In our series, the signal intensity of thrombus on both the T1- and T2-weighted images was similar to those of recently published findings [4, 5]. Mixed signal intensity with a heterogeneous distribution was seen on both T1- and T2-weighted images. In one of these reports [4] thrombus was described as having a multilaminated appearance and a thin inner rim of short T1, high-intensity methemoglobin adjacent to the patent lumen. However, in our study group, a multilaminated thrombus was seen in only one case, and methemoglobin, if present, was never confined to the inner rim. In three of the partially thrombosed aneurysms, an outer short T1 rim was identified. Previous pathologic studies have shown that walls of giant aneurysms are lined by vascularized fibrous tissue, presumably accounting for rim enhancement on contrast CT [27, 28]. Accompanying microscopic hemorrhage in this vascular network also occurs and we speculate that there is methemoglobin deposition, as shown on MR.

The data on low flip angle, gradient-refocused evaluation of intracranial hematomas is still limited. It is predictable that regions of magnetic susceptibility would have decreased intensity on appropriately T2*-weighted images owing to preferential T2 shortening [29]. The parameters used for cine MR imaging in this study are best described as having "some T2* weighting" [23]. However, extensive signal loss in partially thrombosed aneurysms in the pretherapeutic group was not seen even if there was apparent T2 shortening on the routine T2-weighted images. This lack of signal loss may be caused by increased T1-weighting due to the short TE (12.5 msec), relatively long flip angle (30°) or the presence of varying amounts of methemoglobin. Similar to routine T1-weighted images, methemoglobin appears quite bright on the cine MR sequence and may mimic flowing blood. The poor contrast resolution between the high-intensity patent lumen and thrombus is a distinct limitation of cine MR and explains why a small patent lumen was missed in one of the partially thrombosed giant aneurysms in the pretherapy group.

Cine MR may be helpful in therapy planning by further defining the presence and extent of thrombosis, since such thrombi may contribute to distal emboli if clipping or intraaneurysmal balloon embolization is planned [30, 31]. Identification of fresh, nonorganized thrombus may have even greater therapeutic implications, since it is most prone to result in distal emboli. Routine MR images may not be able to predict the age of thrombus [32]. In the pretherapy group, we undoubtedly imaged thrombi of varying ages, thus accounting for the range of intensity seen on both the routine and cine MR studies. Since pathologic correlation was not performed, it was difficult to correlate specific signal characteristics with the age of the thrombus in the pretherapy group. On the other hand, the posttherapeutic patients provided a good in vivo model for evaluating the signal characteristics of thrombus as a function of time, since the exact time course of thrombus formation was known.

Cine MR also has some advantages in posttherapeutic assessment. In patients with ligation of the parent artery, angiography may not completely define a residual lumen if cross-injection of contrast medium is inadequate [9, 33]. Contrast CT was therefore the method of choice for follow-up. Cine MR may provide comparable information. The residual lumen will retain high signal. Confirmation of absent flow within the occluded parent artery as well as detection of collateral filling of distal branches can be obtained simultaneously. In one of our cases, near complete thrombosis of a giant supraclinoid aneurysm was confirmed and pulsatile wall motion had resolved. Despite the fact that the overall size of the aneurysm remained unchanged, there was improvement of the patient's ophthalmoplegia. This finding confirms the hypothesis that pulsatile expansive pressure in addition to the mass itself may contribute significantly to the patient's symptoms [9]. Shrinkage of the aneurysm has been noted on CT months or years after proximal occlusion [9]. We were unable to confirm this finding, since our study was confined to the immediate postoperative period.

In one patient examined with cine MR 24 hr after proximal artery occlusion, fresh thrombus with decreased signal could be seen compared with surrounding, presumably chronic, organized thrombus. This finding was less apparent on the routine T2-weighted images. Acute thrombus is associated with magnetic susceptibility changes caused by the presence of deoxyhemoglobin [29] and a marked decrease in T2 values as measured in vivo [34]. Since low flip angle, gradient-refocused imaging techniques, either gated or nongated, are more sensitive to these differences, it is interesting to speculate that a potential application in detecting acute thrombus exists. More experimental work is needed to confirm this observation.

Distinguishing HEMA-filled balloons from flowing blood is very difficult on routine MR, since both produce a signal void. Polymerized HEMA essentially behaves like a solid with a measured T2 of approximately 5 msec (Guillaumin, Berry, Hieshima, et al., unpublished results) and appears as a signal void on both routine and cine MR images. This technique can detect a residual lumen because flowing blood has high signal intensity on cine MR, and it is now being used on patients who are receiving long-term follow-up evaluation of partially treated aneurysms at our institution.

A variable incidence of parenchymal reaction surrounding the aneurysm, consistent with either edema, atrophy, or ischemia, has been seen with CT [27, 28, 35]. In four patients in our study population, adjacent parenchymal changes were seen on the T2-weighted studies. We are uncertain of the significance of this finding. These changes were not well seen with cine MR, and therefore this technique is not reliable in evaluating intraparenchymal abnormalities. Other current limitations of cine MR include partial volume artifacts and less than optimal spatial resolution. Flow-related enhancement is dependent on the relative volume and uniform velocity of unsaturated spins. It may be decreased by slow or in-plane flow, vasospasm, dilution, and excessive turbulence. Data acquisition may not be possible if there is excessive variation in the R-R interval due to cardiac arrhythmias.

In summary, routine MR is both sensitive and specific in the diagnosis of large and giant intracranial aneurysms. Cine MR provides additional anatomic and physiologic data in the evaluation and assessment of therapy of these lesions. This information cannot be obtained with routine MR, CT, or

angiography. Cine MR appears useful in differentiating thrombus from flow artifact and in documenting turbulence and pulsatile motion and its effect on surrounding parenchyma. Distinction between flowing blood and HEMA-filled balloons within the aneurysm is also possible with this technique. We are now analyzing other intracranial vascular lesions, such as dural arteriovenous fistulas and arteriovenous malformations, as well as occlusion of major arteries and dural sinuses. The inherent limitations of cine MR must be recognized, and it will probably not replace angiography in the near future.

ACKNOWLEDGMENTS

We thank John Smith and Mike Collins for their excellent technical help; Kara Reynolds, Martha Loera, and Rilla Hubbard for manuscript preparation; and the helpful suggestions by Udo Sechtem, Peter Pflugfelder, and Ann Shimakawa of General Electric Medical Systems. We also thank T. Hans Newton and William G. Bradley, Jr., for manuscript review.

REFERENCES

1. Worthington BS, Kean DM, Hawkes RC, Holland GN, Moore WS, Corston R. NMR imaging in the recognition of giant intracranial aneurysms. *AJNR* **1983**;4:835–836
2. Alvarez O, Hyman RA. Even echo MR rephasing in the diagnosis of giant intracranial aneurysms. *J Comput Assist Tomogr* **1986**;10:699–701
3. Camras LR, Reicher MA, Bentson JR, Wilson GH. Partially thrombosed giant aneurysm simulating an arteriovenous malformation on MR imaging. *J Comput Assist Tomogr* **1987**;11:326–328
4. Atlas SW, Grossman RI, Goldberg HI, Hackney DB, Bilaniuk LT, Zimmerman RA. Partially thrombosed giant intracranial aneurysms: correlation of MR and pathologic findings. *Radiology* **1987**;162:111–114
5. Olsen WL, Brant-Zawadzki M, Hodes J, Norman D, Newton TH. Giant intracranial aneurysms: MR imaging. *Radiology* **1987**;163:431–435
6. Bull J. Massive aneurysms at the base of the brain. *Brain* **1969**;92:535–570
7. Pia HW. Large and giant aneurysms. *Neurosurg Rev* **1980**;3:7–16
8. Whittle IR, Dorsch NW, Besser M. Giant intracranial aneurysms: diagnosis, management, and outcome. *Surg Neurol* **1984**;21:218–230
9. Ishii R, Tanaka R, Koike T, et al. Computed tomographic demonstration of the effect of proximal parent artery ligation for giant intracranial aneurysms. *Surg Neurol* **1983**;19:532–540
10. Sechtem U, Pflugfelder PW, White RD, et al. Cine MR imaging: potential for the evaluation of cardiovascular function. *AJR* **1987**;148:239–246
11. Utz J, Herfkens R, Glover G, Shimakawa A, Fram E, Heinsimer J. Rapid dynamic imaging of the heart (abstr). *Proc annual meeting Soc Mag Reson Med*, Montreal, August **1986**:930–931
12. Sechtem U, Pflugfelder PW, Gould RG, Cassidy MM, Higgins CB. Measurement of right and left ventricular volumes in healthy individuals with cine MR imaging. *Radiology* **1987**;163:697–702
13. Haase A, Matthaei D, Hänicke W, Frahm J, Deimling M, Weber H. Time-resolved blood flow and perfusion studies of inner organs using ECG triggered flash NMR movie sequences (abstr). *Proc annual meeting Soc Mag Reson Med*, Montreal, August **1986**:125–126
14. Frahm J, Haase A, Matthaei D. Rapid NMR imaging of dynamic processes using the flash technique. *Magn Reson Med* **1986**;3:321–327
15. Hieshima GB, Higashida RT, Halbach VV, Cahan L, Goto K. Intravascular balloon embolization of a carotid-ophthalmic artery aneurysm with preservation of the parent vessel. *AJNR* **1986**;7:916–918
16. Axel L. Blood flow effects in magnetic resonance imaging. *AJR* **1984**;143:1157–1166
17. Bradley WG, Waluch V. Blood flow: magnetic resonance imaging. *Radiology* **1985**;154:443–450
18. von Schulthess GK, Higgins CB. Blood flow imaging with MR: spin-phase phenomena. *Radiology* **1985**;157:687–695
19. Mills CM, Brant-Zawadzki M, Crooks LE, et al. Nuclear magnetic resonance: principles of blood flow imaging. *AJR* **1984**;142:165–170
20. van Dijk P, Guilfoyle DN, Snaar JEM, Bohning DE. Characterization of flow dynamics by fast multiphase imaging (abstr). *Proc annual meeting Soc Mag Reson Med*, Montreal, August **1986**:625–626
21. Fram E, Hedlund L, Dimick R, Glover G, Herfkens R. Parameters determining the signal of flowing fluid in gradient refocused imaging: flow velocity, TR, and flip angle (abstr). *Proc annual meeting Soc Mag Reson Med*, Montreal, August **1986**:84–85
22. Hearshen DO, Froelich JW, Wherli FW, Haggar AM, Shimakawa A. Time of flight flow effects from gradient recalled echoes with short TR's (abstr). *Proc annual meeting Soc Mag Reson Med*, Montreal, August **1986**:94–95
23. Wehrli FW. *Introduction to fast-scan magnetic resonance* (monograph). Milwaukee: General Electric Medical Systems, **1986**:6
24. Peshock R, Barker B, Katz J, et al. Optimizing small flip angle imaging for the evaluation of cardiovascular structure and function (abstr). *Proc annual meeting Soc Mag Reson Med*, Montreal, August **1986**:64–65
25. Buxton RB, Edelman RR, Rosen BR, Wismer GL, Brady TJ. Contrast in rapid MR imaging: T1- and T2-weighted imaging. *J Comput Assist Tomogr* **1987**;11:7–16
26. Cox IJ, Bydder GM, Gadian DG, et al. The effect of magnetic susceptibility variations in NMR imaging and NMR spectroscopy in vivo. *J Magn Reson* **1986**;70:163–168
27. Pinto RS, Kricheff II, Butler AR, Murali R. Correlation of computed tomographic, angiographic, and neuropathological changes in giant cerebral aneurysms. *Radiology* **1979**;132:85–92
28. Schubiger O, Valavanis A, Hayek J. Computed tomography in cerebral aneurysms with special emphasis on giant intracranial aneurysms. *J Comput Assist Tomogr* **1980**;4:24–32
29. Gomori JM, Grossman RI, Goldberg HI, Zimmerman RA, Bilaniuk LT. Intracranial hematomas: imaging by high field MR. *Radiology* **1985**;157:87–93
30. Hosobuchi Y. Giant intracranial aneurysms. In: Wilkins RH, Rengachary SS, eds. *Neurosurgery*, vol 2. New York: McGraw Hill, **1985**:1408–1412
31. Berenstein A, Ransohoff J, Kupersmith M, Flamm E, Graeb D. Transvascular treatment of giant aneurysms of the cavernous carotid and vertebral arteries. *Surg Neurol* **1984**;21:3–12
32. Erdman WA, Weinreb JC, Cohen JM, Buja LM, Chaney C, Peshock RM. Venous thrombosis: clinical and experimental imaging. *Radiology* **1986**;161:233–238.
33. Pozzati E, Fagioli L, Servadei F, Gaist G. Effect of common carotid ligation on giant aneurysms of the internal carotid artery. *J Neurosurg* **1981**;55:527–531
34. Rapoport S, Sostman HD, Pope C, Camputaro CM, Holcomb W, Gore JC. Venous clots: evaluation with MR imaging. *Radiology* **1987**;162:527–530
35. O'Neill M, Hope T, Thomson G. Giant intracranial aneurysms: diagnosis with special reference to computerized tomography. *Clin Radiol* **1980**;31:27–39